

# Balancing Embedding Spectrum for Recommendation

Shaowen Peng, Kazunari Sugiyama, Xin Liu, and Tsunenori Mine *Member, IEEE*

**Abstract**—Modern recommender systems heavily rely on high-quality representations learned from high-dimensional sparse data. While significant efforts have been invested in designing powerful algorithms for extracting user preferences, the factors contributing to good representations have remained relatively unexplored. In this work, we shed light on an issue in the existing pair-wise learning paradigm (*i.e.*, the embedding collapse problem), that the representations tend to span a subspace of the whole embedding space, leading to a suboptimal solution and reducing the model capacity. Specifically, optimization on observed interactions is equivalent to a low pass filter causing users/items to have the same representations and resulting in a complete collapse. While negative sampling acts as a high pass filter to alleviate the collapse by balancing the embedding spectrum, its effectiveness is only limited to certain losses, which still leads to an incomplete collapse. To tackle this issue, we propose a novel method called DirectSpec, acting as a reliable all pass filter to balance the spectrum distribution of the embeddings during training, ensuring that users/items effectively span the entire embedding space. Additionally, we provide a thorough analysis of DirectSpec from a decorrelation perspective and propose an enhanced variant, DirectSpec<sup>+</sup>, which employs self-paced gradients to optimize irrelevant samples more effectively. Moreover, we establish a close connection between DirectSpec<sup>+</sup> and uniformity, demonstrating that contrastive learning (CL) can alleviate the collapse issue by indirectly balancing the spectrum. Finally, we implement DirectSpec and DirectSpec<sup>+</sup> on two popular recommender models: MF and LightGCN. Our experimental results demonstrate its effectiveness and efficiency over competitive baselines.

**Index Terms**—Recommender System, Collaborative Filtering, Embedding Collapse, Embedding Spectrum

## I. INTRODUCTION

Recommender systems have penetrated into our daily life, we can see them everywhere such as e-commerce [1], short-video [2], social network [3], and so on. Collaborative filtering (CF), a fundamental technique for recommendation to discover user preference based on the historical data, has attracted much attention in the last decades. The most extensively used CF technique, matrix factorization (MF) [4] which represents users and items as low dimensional latent vectors and estimates the rating as the inner product between latent vectors, has been the cornerstone of modern recommender systems. Since MF

estimates the rating with a simple linear function, subsequent works mostly focus on designing more powerful and complex algorithms to model non-linear user-item relations, including but not limited to multi-layer perceptron (MLP) [5], attention mechanism [6], reinforcement learning [7], transformer [8], diffusion model [9] graph neural network (GNN) [10], [11], etc., and have shown tremendous success.

Although different kinds of methods have been proposed, most of them can be considered as MF variants whose goal is to learn low dimensional representations (with dimension  $d$ ) from the high dimensional sparse interaction matrix (with dimension  $D \gg d$ ). Figure 1 illustrates the top 500 normalized singular value distribution of the interaction matrix of CiteULike (see Section 5.1 for data description). We observe that users/items are predominantly distributed along a few dimensions in the original space while most dimensions barely contribute (*i.e.*, with singular values close to 0) to the representations. Thus, when users and items are mapped into a more compact embedding space, it is expected that redundant dimensions are all removed and each dimension contributes to the user/item representations as equally and uniformly as possible (*i.e.*, the representations make full use of the embedding space).

Existing recommendation methods are mostly optimized by pulling observed user-item pairs closer than unobserved ones. Here, a simple yet fundamental question arises: Can user/item representations of existing work make full use of all dimensions? Unfortunately, by analyzing the spectrum of the embedding matrix, we empirically and theoretically show that users/items tend to span a subspace of the whole embedding space (with dimension  $d' < d$ ), where the embeddings collapse along all (complete collapse) or certain dimensions (incomplete collapse). Particularly, optimization solely on observed interactions is equivalent to a low pass filter, where the representations of users and items tend to collapse to a constant vector. Negative sampling is the most common technique to optimize recommendation algorithms without causing an explicit embedding collapse by pushing away the unobserved user-item pairs, and we show that it is equivalent to a high pass filter that decelerates the speed of collapse by balancing the embedding spectrum. However, the effectiveness of negative sampling is only limited to certain loss functions such as Bayesian personalized ranking (BPR) [12] and binary cross-entropy (BCE) loss [5], where collapse over certain dimensions still exists. Due to the data sparsity and long tailed distribution, increasing negative sampling ratios has been shown effective improving the representation quality [5], [13], whereas we also empirically demonstrate

Shaowen Peng is with the Department of Information Science, Nara Institute of Science and Technology, Japan (e-mail: peng.shaowen@naist.ac.jp).

Kazunari Sugiyama is with the Faculty of Data Science, Osaka Seikei University, Japan (e-mail: sugiyama-k@g.osaka-seikei.ac.jp).

Xin Liu is with the Artificial Intelligence Research Center, National Institute of Advanced Industrial Science and Technology, Japan (e-mail: xin.liu@aist.go.jp).

Tsunenori Mine is with Department of Advanced Information Technology, Kyushu University, Japan (e-mail: mine@ait.kyushu-u.ac.jp).

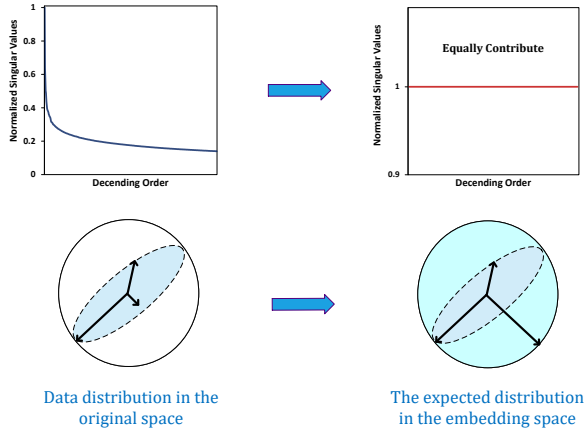


Fig. 1. An illustration of the data distribution in the original space and expected distribution in the learning embedding space.

that it cannot further alleviate the collapse issue by evaluating different negative sampling ratios.

In this work, we tackle the embedding collapse issue from a spectral perspective. We observe that the extent of the collapse is closely related to the spectrum distribution of the embedding matrix. Specifically, only one singular value dominates when the representations completely collapse, whereas the singular values are uniformly distributed when the representations make full use of the embedding space. Inspired by this observation, we propose a novel method dubbed DirectSpec acting as an all pass filter to ensure that all dimensions equally contribute to the representations. We theoretically and empirically show that DirectSpec can completely prevent the embedding collapse without explicitly sampling negative pairs by directly balancing the spectrum distribution, and provide a simple implementation with a complexity only as  $\mathcal{O}(B^2d)$  where  $B$  is the batch size. Moreover, we shed light on DirectSpec from a decorrelation perspective, and propose an enhanced variant DirectSpec<sup>+</sup> which employs self-paced gradients to optimize the irrelevant samples that are highly correlated more effectively. By showing the close connection between DirectSpec<sup>+</sup> and uniformity, we discover that contrastive learning (CL) can alleviate embedding collapse by balancing spectrum distribution in a similar way to DirectSpec, explaining the effectiveness of CL based recommendation algorithms. Finally, we implement DirectSpec and DirectSpec<sup>+</sup> on two popular baselines: MF [4] and LightGCN [14]. Experimental results show that DirectSpec<sup>+</sup> improves BPR and LightGCN by up to 52.6% and 41.8% in terms of nDCG@10, respectively. The contribution of this work can be summarized as follows:

- We theoretically and empirically show that existing recommendation methods suffer from embedding collapse, that the representations tend to fall into a subspace of the whole embedding space, and analyze the causes behind this issue.
- We propose a novel method dubbed DirectSpec which acts as an all pass filter to directly balance the embedding spectrum. We empirically and theoretically show that DirectSpec can prevent embedding collapse.

- We unveil the effectiveness of CL by showing that uniformity, a key design of CL can alleviate collapse issue by indirectly balancing the spectrum distribution that can be considered as a special case of DirectSpec.
- Extensive results on three datasets demonstrate the efficiency and effectiveness of our proposed methods.

## II. PRELIMINARIES

### A. Pairwise Learning for CF

Given the user set  $\mathcal{U}$  and item set  $\mathcal{I}$ , the interaction matrix is defined as  $\mathbf{R} \in \{0, 1\}^{|\mathcal{U}| \times |\mathcal{I}|}$ , the observed interactions are represented as  $\mathbf{R}^+ = \{r_{ui} = 1 | u \in \mathcal{U}, i \in \mathcal{I}\}$ . Users and items are first mapped to low dimensional vectors  $\mathbf{H} \in \mathbb{R}^{(|\mathcal{U}|+|\mathcal{I}|) \times d}$  through an encoder, where the encoder can be as simple as a linear mapping [4] or advanced algorithms such as MLPs [5], GNNs [15], etc. Let  $\mathbf{h}_u$  and  $\mathbf{h}_i$  be the  $u$ 's and  $i$ 's representations, respectively. The goal of CF is to predict unobserved interactions  $\mathbf{R}^- = \{r_{ui} = 0 | u \in \mathcal{U}, i \in \mathcal{I}\}$  estimated as the inner product between the user and item representations:  $\hat{r}_{ui} = \mathbf{h}_u^T \mathbf{h}_i$ . The model parameters  $\Theta$  are optimized through a loss function  $\mathcal{L}$  formulated as follows:

$$\arg \min_{\Theta} \mathcal{L}(\hat{r}_{ui}, r_{ui}). \quad (1)$$

The loss function measures the difference between the estimated score and the ground truth. BPR and BCE loss are two extensively used learning frameworks for CF methods:

$$\begin{aligned} \mathcal{L}_{BPR} &= \sum_{(u,i) \in \mathbf{R}^+, (u,j) \in \mathbf{R}^-} -\ln \sigma(\hat{r}_{ui} - \hat{r}_{uj}), \\ \mathcal{L}_{BCE} &= \sum_{u \in \mathcal{U}, i \in \mathcal{I}} -r_{ui} \ln \sigma(\hat{r}_{ui}) - (1 - r_{ui}) \ln (1 - \sigma(\hat{r}_{ui})), \end{aligned} \quad (2)$$

where  $\sigma(\cdot)$  is the sigmoid function. BPR loss maximizes the difference between observed and unobserved user-item pairs, while BCE loss directly pulls the observed pairs close and pushes the unobserved ones away from each other. The embeddings are a low dimensional approximation of the sparse high dimensional interaction matrix, thus they should contain diverse and rich information representing the user-item relations. Rank is a commonly used metric to measure the dimension of a matrix, while it fails to tell the difference between the embedding matrix (1) with a ‘sphere’ distribution that users/items are uniformly distributed in each dimension of the space and (2) with a ‘spheroid’ distribution that users/items are predominantly distributed over some dimensions and insignificantly distributed over other dimensions. Although both matrices have the same rank, apparently (1) contains more diverse information than (2). Here, we introduce another tool:

**Definition 1. Effective Rank.** Given singular values of the embedding matrix  $\mathbf{H}$ :  $\sigma_1 \geq \sigma_2 \geq \dots \geq \sigma_d \geq 0$ , let  $p_k = \frac{\sigma_k}{\sum_k \sigma_k}$ , then the effective rank is defined as follows:

$$\text{erank}(\mathbf{H}) = \exp(H(p_1, \dots, p_d)), \quad (3)$$

where  $H(p_1, \dots, p_d) = -\sum_k p_k \log p_k$  is the Shannon entropy.

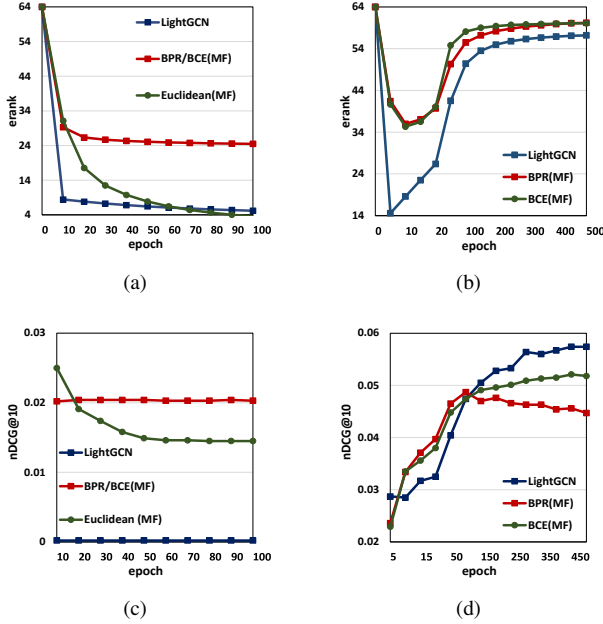


Fig. 2. Embedding collapse on Yelp ( $d = 64$ ). (a) and (b) show how embeddings completely and incompletely collapse, respectively; (c) and (d) show how nDCG@10 changes as the training proceeds under the two situations.

Compared with rank,  $erank$  takes the singular value distribution into consideration: the more uniform (sharper) of the distribution, the higher (lower) of the  $erank$  [16]. The embedding matrix contains the least information when there is only one leading non-zero singular values ( $\sigma_2 = \dots = \sigma_d = 0$ , and  $erank(\mathbf{H}) = rank(\mathbf{H}) = 1$ ), while  $erank$  is maximized when each dimension equally contributes to the representations:  $\sigma_1 = \dots = \sigma_d$  ( $erank(\mathbf{H}) = rank(\mathbf{H}) = d$ ).

### B. Graph Representation and Graph Filtering

The interactions can be represented as a graph. Consider a graph  $\mathcal{G} = (\mathcal{V}, \mathcal{E}, \mathbf{A})$ , where the node set contains all users and items:  $\mathcal{V} = \mathcal{U} \cup \mathcal{I}$ , the edge set is represented by observed interactions:  $\mathcal{E} = \mathbf{R}^+$ ,  $\mathbf{A}$  is an adjacency matrix. Suppose  $\mathbf{A}$  is normalized with the eigenvalue  $|\lambda_k| \leq 1$ , then:

**Definition 2. Graph Filtering.** Let  $1 = \lambda_1 > \lambda_2 > \dots > \lambda_n = -1$  be the eigenvalues of  $\mathbf{A}$  where  $n = |\mathcal{V}|$ . The component closer to  $\lambda_1$  and  $\lambda_n$  correspond to a lower and higher frequency, respectively.  $\mathcal{F}^L(\mathbf{A})$  is a low pass filter if  $|\mathcal{F}^L(\lambda_i)| > |\mathcal{F}^L(\lambda_j)|$  for  $\lambda_i > \lambda_j$  and  $\mathcal{F}^H(\mathbf{A})$  is a high pass filter if  $|\mathcal{F}^H(\lambda_i)| > |\mathcal{F}^H(\lambda_j)|$  for  $\lambda_i < \lambda_j$ .

Note that  $\mathcal{F}^L(\mathbf{A})$  is defined as a low pass filter as it emphasizes more on the lower frequencies and similarly for the definition for high pass filters. Please refer to [17] for detailed introduction of graph frequency.

## III. EMBEDDING COLLAPSE IN CF

### A. Complete Collapse

Let us first consider a extensively used loss function in recommendation: log loss. Here, we only optimizes the observed interactions:  $\mathcal{L} = -\sum \ln \sigma(\hat{r}_{ui}), (u, i) \in \mathbf{R}^+$ .

**Proposition 1.** Suppose  $G$  is connected, then  $\mathbf{h}_k \approx \mathbf{h}_z$  for arbitrary nodes  $k$  and  $z$  when  $\mathcal{L}$  completely converges.

By calculating the gradient over the embeddings, the parameters are updated through stochastic gradient descent (SGD) as follows:

$$\begin{aligned} \mathbf{H}^{(l+1)} &= \mathbf{H}^{(l)} - \alpha \frac{\partial \mathcal{L}}{\partial \mathbf{H}^{(l)}} = \mathbf{H}^{(l)} + \alpha \mathbf{A} \mathbf{H}^{(l)}, \\ \mathbf{h}_u^{(l+1)} &= \mathbf{h}_u^{(l)} - \alpha \frac{\partial \mathcal{L}}{\partial \mathbf{h}_u^{(l)}} = \mathbf{h}_u^{(l)} + \alpha \sum_{(u,i) \in \mathbf{R}^+} \mathbf{A}_{ui} \mathbf{h}_i^{(l)}, \end{aligned} \quad (4)$$

where  $\alpha \in (0, 1)$ ,  $\mathbf{A}_{ui} = 1 - \sigma(\hat{r}_{ui})$  for  $(u, i) \in \mathbf{R}^+$ . Equation (4) is similar to the message passing in GNN [18], which makes the nodes similar to their neighborhood. Repeating Equation (4) multiple times can further reach the higher-order neighborhood, causing indirectly connected nodes to be similar. While  $\mathbf{A}_{ui}$  controlling the magnitude of the gradient tends to vanish as training proceeds, and eventually  $\mathcal{L}$  converges when  $\mathbf{A}$  degenerates into a zero matrix. Note that this issue does not exist on other loss functions such as Euclidean distance loss:  $\sum \|\mathbf{h}_u - \mathbf{h}_i\|_2^2$  with fixed magnitude of gradients, where Equation (4) can be rewritten as:

$$\mathbf{H}^{(l)} = (\mathbf{I} + \alpha \mathbf{A})^l \mathbf{H}^{(0)}. \quad (5)$$

Suppose  $\mathbf{A}$  is normalized such as  $|\lambda_k| \leq 1$ , then  $(\mathbf{I} + \alpha \mathbf{A})^l$  is equivalent to a low pass filter, as the eigenvalue of  $\mathbf{I} + \alpha \mathbf{A}$  is  $1 + \alpha \lambda_k \in [1 - \alpha, 1 + \alpha]$  with  $1 - \alpha > 0$  and  $x^l$  is monotonically increasing for  $l > 0$  and  $x > 0$ . According to the spectral decomposition with  $\mathbf{v}_k$  as the eigenvector:

$$(\mathbf{I} + \alpha \mathbf{A})^l = \sum_k (1 + \alpha \lambda_k)^l \mathbf{v}_k \mathbf{v}_k^T, \quad (6)$$

it is obvious that  $\frac{(1 + \alpha \lambda_k)^l}{(1 + \alpha \lambda_1)^l} \rightarrow 0$  ( $k \neq 1$ ) as  $l$  is large enough, resulting in  $rank((\mathbf{I} + \alpha \mathbf{A})^l) \rightarrow 1$ , then:

$$rank(\mathbf{H}^{(l)}) \leq \min(rank((\mathbf{I} + \alpha \mathbf{A})^l), rank(\mathbf{H}^{(0)})) = 1, \quad (7)$$

showing that all nodes have the same embedding representations. Considering that the gradient vanishing hinders the convergence of Equation (5), the representations of distinct nodes would not be completely the same on the log loss.

In Figure 2 (a) and (c), we evaluate LightGCN and MF on how the embeddings completely collapse on Yelp when only considering the observed interactions, the parameters are initialized with Xavier initialization. Furthermore, we adopt a Euclidean distance loss implemented on MF without the gradient vanishing issue. We have the following observations:

- Before the training starts, the embeddings are uniformly distributed in the embedding space since  $erank(\mathbf{H}) \approx d$ .
- The  $erank$  monotonically decreases on all models, and the accuracy barely changes throughout the training, indicating that the embeddings collapse as the training starts and the issue becomes more serious as training proceeds.
- The  $erank$  decreases more rapidly on LightGCN than MF. Consider a  $K$ -layer LightGCN, then Equation (5) can be rewritten as:

$$\mathbf{H}^{(l)} = (\mathbf{I} + \alpha \mathbf{A})^l \sum_{k=0}^{K-1} \mathbf{A}^k \mathbf{E}. \quad (8)$$

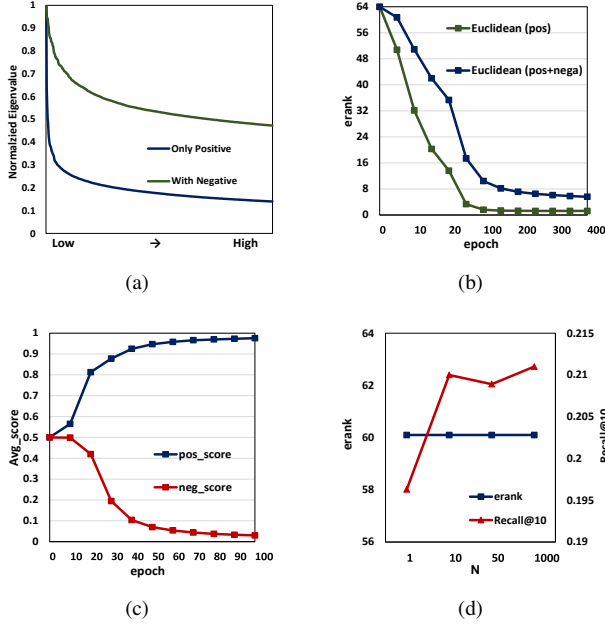


Fig. 3. Some analysis on CiteULike. (a) the normalized eigenvalue distribution (Top 500) of  $\mathbf{A} - \bar{\mathbf{A}}$ ; (b) how erank changes on Euclidean distance loss optimizing only positive and both positive and negative samples; (c) how the average scores of sampled positive negative pairs change with training; (d) how erank and recall@10 change with varying negative sampling ratios.

Here,  $\mathbf{E}$  is the initial stacked user/item embeddings sent to the encoder; we ignore the difference between the adjacency matrix used in Equation (5) and LightGCN for simplicity. We can see that increasing the layer  $K$  causes the loss function to converge faster, indicating that the over-smoothing in GNN [19] aggravates the collapse issue.

- The erank tends to converge to a value larger than 1. Besides the gradient vanishing mentioned above, Proposition 1 is based on the assumption that  $\mathcal{G}$  is connected, which does not always hold on the real-world datasets. In other words, disconnected nodes (*i.e.*, no reachable paths between them) do not end up having the same representations.
- By comparing the Euclidean distance loss (MF) and log loss (MF), we can see the erank of Euclidean distance loss with fixed magnitude of gradients whose accuracy is also worse drops more quickly than that of log loss, which further verifies our analysis.

## B. Incomplete Collapse

Existing recommendation algorithms mostly exploit unobserved interactions for optimization. Naturally, we raise a question: Can existing pair-wise learning paradigm completely prevent the collapse? Similarly, we evaluate LightGCN (with BPR), MF (with BPR), and MF (with BCE) on Yelp, and show how erank and accuracy change as training proceeds in Figure 2 (b) and (d). The erank plunges at first, showing a trend similar to Figure 2 (a). Gradually, the erank increases and tends to converge to a value lower than  $d$ , indicating that the embeddings are negligibly distributed over some dimensions. LightGCN drops more rapidly than MF and converges to a smaller value. In the meanwhile, the accuracy also increases

accordingly, and shows a trend similar to erank. It is obvious that existing algorithms (BCE and BPR loss) can alleviate the collapse issue but still cannot completely prevent it. We attempt to analyze how they alleviate the collapse issue and the weakness. Take the BCE loss as an example, the parameters are updated through SGD as follows:

$$\begin{aligned} \mathbf{H}^{(l+1)} &= \mathbf{H}^{(l)} + \alpha (\mathbf{A} - \bar{\mathbf{A}}) \mathbf{H}^{(l)}, \\ \mathbf{h}_u^{(l+1)} &= \mathbf{h}_u^{(l)} + \alpha \sum_{(u,i) \in \mathbf{R}^+} \mathbf{A}_{ui} \mathbf{h}_i^{(l)} - \alpha \sum_{(u,j) \in \mathbf{R}^-} \bar{\mathbf{A}}_{uj} \mathbf{h}_j^{(l)}, \end{aligned} \quad (9)$$

where  $\bar{\mathbf{A}}_{uj} = \sigma(\hat{r}_{uj})$  for  $(u, j) \in \mathbf{R}^-$ . As the direction of the gradient is opposite to that of observed interactions, it seems that the disconnected nodes (unobserved interactions) are pushed away from the target users/items, preventing the representations from collapsing.

However, we now show that negative sampling alone is actually not able to avoid the complete collapse. Ideally, with the magnitude of gradient fixed, Equation (9) can be rewritten to the following Equation similar to Equation (5):

$$\mathbf{H}^{(l)} = (\mathbf{I} + \alpha (\mathbf{A} - \bar{\mathbf{A}}))^l \mathbf{H}^{(0)}. \quad (10)$$

Here,  $\mathbf{I} + \alpha (\mathbf{A} - \bar{\mathbf{A}})$  can be disentangled to a low pass  $\mathbf{I} + \alpha \mathbf{A}$  and a high pass filter  $\mathbf{I} - \alpha \bar{\mathbf{A}}$ , where a high pass filter can balance the embeddings spectrum by reducing the weights on low frequency and raising the importance of high frequency components, leading to a more uniform distribution. We visualize the spectrum of  $\mathbf{A} - \bar{\mathbf{A}}$  in Figure 3 (a), where we fix the elements of  $\mathbf{A}$  and  $\bar{\mathbf{A}}$  to 1 and normalize them separately.  $\bar{\mathbf{A}} = 0$  (zero matrix) for ‘Only positive’, and  $\bar{\mathbf{A}}$  contains all unobserved interactions for ‘With negative’. It is obvious that  $\mathbf{A} - \bar{\mathbf{A}}$  has a more balanced spectrum than  $\mathbf{A}$ , leading to a higher erank. However, according to our previous analysis in Section III-A, the largest eigenvalue still would dominate while other smaller eigenvalues are filtered out as updating the algorithm enough times (*i.e.*,  $\frac{(1+\alpha\lambda_k)^l}{(1+\alpha\lambda_1)^l} \rightarrow 0$  ( $k \neq 1$ )) as long as the spectrum of  $\mathbf{I} + \alpha (\mathbf{A} - \bar{\mathbf{A}})$  is not completely uniform, resulting in a complete collapse. To verify our analysis, we adopt Euclidean distance loss whose magnitude of gradients does not change with training, and show how the erank changes on the model with only positive and both positive and negative samples in Figure 3 (b). We can observe that the erank of the model exploiting negative samples still monotonically declines, regardless of a slower speed than the model with only positive samples. Then, another question rises: What enables BCE and BPR loss to avoid the complete collapse?

As shown in Figure 2 (c), the term controlling the magnitude of the gradient over the positive sample  $\mathbf{A}_{ui}$ :  $1 - \sigma(\hat{r}_{ui})$  is way larger than 0 at the beginning of training, causing the embeddings to collapse. Since positive pairs are more likely to be sampled due to the data sparsity, the gradients vanish faster as they are pulled close:  $\mathbf{A} \rightarrow 0$ , allowing the high pass filter to balance the spectrum. Then, negative samples being pushed away also leads to  $\bar{\mathbf{A}} \rightarrow 0$ , making the representations converge:  $\mathbf{H}^{(l+1)} = \mathbf{H}^{(l)}$  and leading to an incomplete collapse. Furthermore, since it has been shown that raising the negative samples leads to a desirable

TABLE I  
A TOY EXAMPLE DEMONSTRATING THE EFFECTIVENESS OF ALGORITHM 1. THE MATRIX IS RANDOMLY GENERATED WITH A SIZE 10. WITHOUT SPECIFICATION,  $T = 50$ ,  $\alpha = 1e-3$ , AND  $L = 1$ .

$T$	0	1	10	100	500	1000
erank	7.64	7.72	8.11	8.59	9.57	9.75
$\alpha$	0	1e-3	2e-3	5e-3	1e-2	2e-2
erank	7.64	8.43	8.71	9.09	9.35	9.59
$L$	0	1	2	3	-	-
erank	7.64	7.80	8.45	8.83	-	-

representation and improvement [5], [13], we evaluate BCE with different negative sampling ratios and report the results in Figure 3 (c). We can see that the accuracy increases by raising the sampling ratio, while the erank remains unchanged, showing that introducing more negative samples fails to further alleviate or prevent the embedding collapse. To conclude, gradient vanishing on log loss (including BCE and BPR loss) is the ‘X factor’ to prevent the complete collapse, and is also the reason causing the incomplete collapse as well. Therefore, a more effective design proved to completely solve the collapse issue is required.

#### IV. METHODOLOGY

##### A. Balancing Embedding Spectrum

The spectrum distribution can directly reflect the extent of embedding collapse. Intuitively, a uniform distribution indicates that different dimensions equally contribute to the embeddings and leads to a high effective rank. Therefore, a reliable solution is an all pass filter  $\mathcal{F}^A$  such that  $\mathcal{F}^A(\sigma_i) = \mathcal{F}^A(\sigma_j)$  for  $\sigma_i \neq \sigma_j$ . By parameterizing  $\mathcal{F}^A$ , it is straightforward to directly balance the spectrum by optimizing the following loss:

$$\min \sum_{k \neq z} \|\sigma'_k - \sigma'_z\|_2^2, \quad (11)$$

where  $\sigma'_k$  is the singular value of  $\mathcal{F}^A(\mathbf{H})$ . However, such a design requires the computation of singular values during each training and introduces more model parameters that might hinder the model convergence, thus we stick to a simple yet effective design in this work. Consider an affinity graph  $\mathcal{G}' = (\mathcal{V}, \hat{\mathbf{A}})$ , where the node features are represented by the embedding matrix  $\mathbf{H}$  and the adjacency relation is measured by the similarity score between nodes:  $\hat{\mathbf{A}}_{ui} = \mathbf{h}_u^T \mathbf{h}_i$ , we define the message passing on  $\mathcal{G}'$  as follows:

$$\mathcal{F}^A(\mathbf{H}) = \mathbf{H} - \alpha \hat{\mathbf{A}}^L \mathbf{H}, \quad (12)$$

where  $\alpha \in \mathbb{R}^+$ ,  $L \in \mathbb{N}$  is the matrix power.

**Proposition 2.**  $\overbrace{\mathcal{F}^A \dots \mathcal{F}^A}^T(\mathbf{H})$  (Repeating  $\mathcal{F}^A(\mathbf{H})$   $T$  times) is equivalent to an all pass filter where  $\text{erank}(\overbrace{\mathcal{F}^A \dots \mathcal{F}^A}^T(\mathbf{H})) = d$ .

---

##### Algorithm 1: Balancing Embedding Spectrum via Message Passing on $\mathcal{G}'$

---

**Input:** Embedding matrix  $\mathbf{H}$ ; matrix power  $L$ ; the number of iteration  $T$ ; scaling hyperparameter  $\alpha \in \mathbb{R}^+$   
**for**  $t = 1$  **to**  $T$  **do**  
 $\mathbf{H} \leftarrow \mathbf{H} - \alpha \hat{\mathbf{A}}^L \mathbf{H}$ ;  
**end**  
**Return**  $\mathbf{H}$

---



---

##### Algorithm 2: DirectSpec

---

**Input:** Embedding matrix  $\mathbf{H}$ ; batch size  $B$ ; scaling hyperparameter  $\alpha \in \mathbb{R}^+$   
sample the users and items:  $\mathcal{U}_B, \mathcal{I}_B$  ;  
generate the normalized embeddings:  $\mathbf{H}_B^U, \mathbf{H}_B^I$ ;  
 $\mathbf{H}_B^U \leftarrow \mathbf{H}_B^U - \alpha \mathbf{H}_B^U \mathbf{H}_B^{U^T} \mathbf{H}_B^U$ ;  
 $\mathbf{H}_B^I \leftarrow \mathbf{H}_B^I - \alpha \mathbf{H}_B^I \mathbf{H}_B^{I^T} \mathbf{H}_B^I$ ;  
**Return**  $\mathbf{H}_B^U, \mathbf{H}_B^I$

---

We can rewrite Equation (12) according to singular value decomposition (SVD) as follows:

$$\begin{aligned} \mathcal{F}^A(\mathbf{H}) &= \mathbf{H} - \alpha (\mathbf{H}\mathbf{H}^T)^L \mathbf{H} \\ &= \mathbf{P} \text{diag}(\sigma_k) \mathbf{Q}^T - \alpha \mathbf{P} \text{diag}(\sigma_k^{2L+1}) \mathbf{Q}^T \quad (13) \\ &= \mathbf{P} \text{diag}(\sigma_k (1 - \alpha \sigma_k^{2L})) \mathbf{Q}^T, \end{aligned}$$

where  $\mathbf{P}$  and  $\mathbf{Q}$  are stacked singular vectors,  $\text{diag}(\cdot)$  is the diagonalization operation. It is obvious that  $1 - \alpha \sigma_i^{2L} > 1 - \alpha \sigma_j^{2L}$  for  $\sigma_i < \sigma_j$ . Thus  $1 - \alpha \sigma_k^{2L}$  can be considered as rescaled factors: the larger singular values corresponding to the lower frequency components are multiplied by smaller weights, leading to a more uniform distribution when  $L > 0$ .  $L$  and  $\alpha$  control the weight multiplied on the singular value of  $\mathbf{H}$ , thus directly affect the efficiency of spectrum balancing. A larger (smaller)  $L$  makes the rescaled factors smaller (larger) on the large singular values, and  $\alpha$  controls the norms of the rescaled factors that has a similar effect to  $L$ . Since  $\sigma_k^L$  increases fast, a large  $L$  could reduce the algorithm’s efficiency where the large singular values in the original distribution are multiplied by too small weights, causing a sharp singular value distribution similar to the original one. In addition, too large  $L$  or  $\alpha$  could also break the non-negativity of the singular value, thus we need to assure that  $1 - \alpha \sigma_1^{2L} > 0$ . According to the definition of Entropy and erank, a more uniform distribution results in a larger erank, indicating that  $\text{erank}(\mathcal{F}^A(\mathbf{H})) \geq \text{erank}(\mathbf{H})$  where  $=$  holds when  $\text{erank}(\mathbf{H}) = d$ . By sufficiently repeating Equation (13), eventually  $\text{erank}(\mathbf{H}) = d$ . We summarize the above analysis and propose Algorithm 1 to tackle the embedding collapse. We run Algorithm 1 on a randomly generated matrix with the code `torch.randn(10,10)`<sup>1</sup>, and report the results with different settings of  $\alpha$ ,  $L$ , and  $T$  in Table I, where  $1 - \alpha \sigma_1^{2L} < 0$  when  $L > 3$ . We can see that the erank tends to converge to  $d = 10$  as we increase the iteration  $T$ , scaling hyperparameter  $\alpha$ , and the order  $L$ ,

<sup>1</sup><https://pytorch.org/>

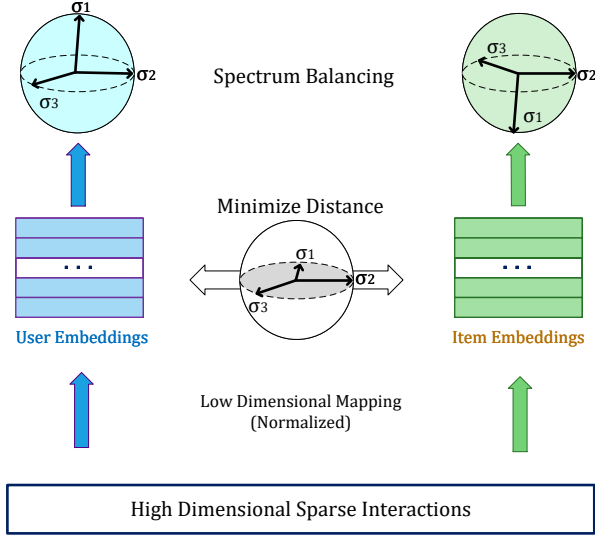


Fig. 4. An illustration of the proposed DirectSpec.

demonstrating the effectiveness of Algorithm 1 balancing the embedding spectrum.

Algorithm 1 is impractical since the complexity is  $\mathcal{O}(TLD^2d)$  where  $D = |\mathcal{U}| + |\mathcal{I}|$ . We propose a simplified implementation of DirectSpec formulated in Algorithm 2. Since the singular value increases fast with  $L$  which could break the non-negativity of the singular value, and in practice we do not need the erank to strictly be  $d$  (we will explain in Section IV-C), we can set  $T = 1$  and  $L = 1$ . In addition, instead of updating the whole embedding matrix, we iteratively rebalance the spectrum of a smaller matrix with a size in accordance with the batch size.

### B. A Decorrelation Perspective

In this subsection, we show how users and items are represented in the embedding space through our proposed DirectSpec from a spatial perspective.

**Proposition 3.** *Algorithm 2 is equivalent to optimizing the following loss:*

$$L_{ds} = \sum_{u \in \mathcal{U}} \sum_{v \in \mathcal{U}} \|\mathbf{h}_u^T \mathbf{h}_v\|^2 + \sum_{i \in \mathcal{I}} \sum_{j \in \mathcal{I}} \|\mathbf{h}_i^T \mathbf{h}_j\|^2. \quad (14)$$

By calculating the gradient over user and item embeddings:

$$\frac{\partial L_{ds}}{\partial \mathbf{h}_u} = 4 \sum_v (\mathbf{h}_u^T \mathbf{h}_v) \mathbf{h}_v, \quad \frac{\partial L_{ds}}{\partial \mathbf{h}_i} = 4 \sum_j (\mathbf{h}_i^T \mathbf{h}_j) \mathbf{h}_j, \quad (15)$$

the parameter updating through SGD can be formulated as follows:

$$\begin{aligned} \mathbf{H}_U &\leftarrow \mathbf{H}_U - \alpha (\mathbf{H}_U \mathbf{H}_U^T) \mathbf{H}_U, \\ \mathbf{H}_I &\leftarrow \mathbf{H}_I - \alpha (\mathbf{H}_I \mathbf{H}_I^T) \mathbf{H}_I, \end{aligned} \quad (16)$$

where  $\mathbf{H}_U$  and  $\mathbf{H}_I$  are user and item embedding matrices, respectively. Therefore, Equation (14) is equivalent to DirectSpec. Intuitively, two users/items are (positively or negatively) correlated if  $|\mathbf{h}_u^T \mathbf{h}_v| > 0$  or  $|\mathbf{h}_i^T \mathbf{h}_j| > 0$ , then we can see that the goal of Equation (14) is to decorrelate/orthogonalize

different users and items (e.g.,  $\mathbf{h}_u^T \mathbf{h}_v \rightarrow 0$  and  $\mathbf{h}_i^T \mathbf{h}_j \rightarrow 0$ ) instead of simply pushing them away.

**Proposition 4.** *The lower bound of  $L_{ds} \rightarrow 0$  as  $d \rightarrow \max(|\mathcal{U}|, |\mathcal{I}|)$ .*

We can see that different users/items are orthogonal to each other when  $L_{ds} = 0$ . Then, consider the following linear combination:

$$\alpha_1 \mathbf{h}_1 + \dots + \alpha_n \mathbf{h}_n = 0. \quad (17)$$

By multiplying Equation (17) by  $\mathbf{h}_k^T$ , we get  $\alpha_k = 0$ , indicating that orthogonal vectors are linearly independent as well, requiring  $d \geq \max(|\mathcal{U}|, |\mathcal{I}|)$ .

From a different perspective,  $\mathbf{H}_U \mathbf{H}_U^T$  and  $\mathbf{H}_I \mathbf{H}_I^T$  represent the similarity scores between users and items, respectively, and we have the following relations according to SVD:

$$\mathbf{H}_U \mathbf{H}_U^T = \mathbf{P} \text{diag}(\sigma_k^2) \mathbf{P}^T, \quad \mathbf{H}_I \mathbf{H}_I^T = \mathbf{Q} \text{diag}(\sigma_k^2) \mathbf{Q}^T. \quad (18)$$

For simplicity, we use the same notations denoting singular values and vectors of  $\mathbf{H}_U$  and  $\mathbf{H}_I$ , since we do not emphasize their difference here. In the meanwhile,  $\mathbf{P}$  and  $\mathbf{Q}$  are also the eigenvectors of  $\mathbf{H}_U$  and  $\mathbf{H}_I$ , respectively. Let  $\lambda_k$  denote the eigenvalue of  $\mathbf{H}_U \mathbf{H}_U^T$  and  $\mathbf{H}_I \mathbf{H}_I^T$ , we have  $\lambda_k = \sigma_k^2$ . When  $(\mathbf{H}_U \mathbf{H}_U^T)_{uv} \rightarrow 0$  and  $(\mathbf{H}_I \mathbf{H}_I^T)_{ij} \rightarrow 0$ ,  $(\mathbf{H}_U \mathbf{H}_U^T)$  and  $(\mathbf{H}_I \mathbf{H}_I^T)$  are optimized to be identity matrices with uniform spectrum distributions:  $\lambda_1 = \lambda_2 = \dots = 1$ , thus  $\mathbf{H}_U$ 's and  $\mathbf{H}_I$ 's spectra are also uniform, leading to a maximum erank. The above observations reveal that unobserved pairs should stay irrelevant instead of simply being pushed away like BCE and BPR loss, which is more consistent with users' true preference over unobserved interactions. We will empirically compare DirectSpec and negative sampling in Section V-B3.

### C. DirectSpec<sup>+</sup>

As the observed pairs should be deeply correlated, perfect user/item decorrelation is not the goal of personalized recommendation, explaining why we do not need (1) the erank of the embedding to strictly be  $d$  and (2)  $d$  to be large enough to reach the perfect decorrelation. The training objective should balance between user/item correlation and decorrelation:

$$L = \sum_{(u,i) \in \mathbf{R}^+} \ln \sigma(\mathbf{h}_u^T \mathbf{h}_i) + L_{ds}. \quad (19)$$

The first term pulls users/items to be close to each other, while the second term offsets the negative effect from the first term by orthogonalizing them. From Equation (15), we can see that all samples are optimized with the same pace. To enhance the efficiency, we can employ self-paced gradients according to the extent of correlation (e.g.,  $\mathbf{h}_u^T \mathbf{h}_v \rightarrow 1$  and  $\mathbf{h}_i^T \mathbf{h}_j \rightarrow 1$  should be penalized more) by improving Equation (14) as:

$$L_{ds} = \sum_{u \in \mathcal{U}} \sum_{v \in \mathcal{U}} \exp(\mathbf{h}_u^T \mathbf{h}_v / \tau) + \sum_{i \in \mathcal{I}} \sum_{j \in \mathcal{I}} \exp(\mathbf{h}_i^T \mathbf{h}_j / \tau). \quad (20)$$

Compared with Equation (15), the pairs with  $\mathbf{h}_u^T \mathbf{h}_v \rightarrow 1$  and  $\mathbf{h}_i^T \mathbf{h}_j \rightarrow 1$  are pushed away at a faster pace (i.e., larger gradients);  $\tau$  is a temperature controlling the strength of penalties. We focus on penalizing the positive correlation

as optimization on the observed interactions causes user/item pairs to be positively correlated. Note that Equation (20) is equivalent to a pairwise Gaussian potential:  $\exp\left(\frac{\mathbf{h}_u^T \mathbf{h}_v}{\tau}\right) = \exp\left(\frac{-\|\mathbf{h}_u - \mathbf{h}_v\|^2}{2\tau} + \frac{1}{\tau}\right)$ , where the minimum is reached when user/item embeddings are orthogonal to each other when  $d$  is large enough according to Proposition 3 in [20]. Thus, the training objective of the enhanced algorithm is consistent with the original DirectSpec. Furthermore, we notice that some unobserved pairs are correlated as well to some extent, such as the users showing similar preference or items interacted by similar users that should be decorrelated with a slower pace than other irrelevant pairs. Here, we propose two adaptive temperature designs to adapt to the pairs with different degrees of correlations:

- i. We dynamically learn the temperature through an attention mechanism such as  $\Gamma_{uv} = \sigma(\mathbf{W}^T[\mathbf{h}_u \parallel \mathbf{h}_v])$  for  $u$  and  $v$ , where  $\parallel$  stands for the concatenate operation and  $\mathbf{W} \in \mathbb{R}^{2d}$  is the transform matrix.
- ii. We define the graph distance between two nodes:  $d_G(\cdot, \cdot)$  as the minimum length of path between them on  $\mathcal{G}$ , then an unparameterized design is defined as follows:

$$\Gamma_{uv} = \begin{cases} \tau_0 & d_G(u, v) \leq K \\ \tau_1 & \text{otherwise,} \end{cases} \quad (21)$$

where the pairs with  $d_G(u, v) \leq K$  are considered correlated, and  $\tau_0 \leq \tau_1$ .

By calculating the gradients of Equation (20), we can incorporate its parameter-updating formula into Algorithm 2, and propose DirectSpec<sup>+</sup>:

$$\begin{aligned} \mathbf{H}_B^U &\leftarrow \mathbf{H}_B^U - \alpha \cdot \text{softmax}\left(\mathbf{H}_B^U \mathbf{H}_B^{U^T} \odot \Gamma\right) \mathbf{H}_B^U, \\ \mathbf{H}_B^I &\leftarrow \mathbf{H}_B^I - \alpha \cdot \text{softmax}\left(\mathbf{H}_B^I \mathbf{H}_B^{I^T} \odot \Gamma\right) \mathbf{H}_B^I. \end{aligned} \quad (22)$$

To regulate the magnitude of the gradient, we rewrite it as a Softmax function. Other steps of DirectSpec<sup>+</sup> are consistent with Algorithm 2.

#### D. Discussion

1) *Connection and Comparison Between DirectSpec<sup>+</sup> and Uniformity Loss:* Contrastive learning (CL) has shown great potential in recommender systems [21], [22], which adopts an InfoNCE loss:

$$L_{cl} = - \sum_u \ln \frac{\exp(\mathbf{h}_u^T \mathbf{h}_{u^+} / \tau)}{\sum_v \exp(\mathbf{h}_u^T \mathbf{h}_v / \tau)} - \sum_i \ln \frac{\exp(\mathbf{h}_i^T \mathbf{h}_i / \tau)}{\sum_j \exp(\mathbf{h}_i^T \mathbf{h}_j / \tau)}, \quad (23)$$

that can be decoupled to alignment and uniformity loss. Alignment minimizes the distance between positive pairs (*i.e.*,  $(u, u^+)$  and  $(i, i^+)$ ). In the meanwhile, embeddings from different users/items are pushed away via uniformity loss, which has been shown necessary for desirable user/item representations [23], [24]. To unveil the effectiveness of uniformity, we fix alignment:  $\mathbf{h}_u^T \mathbf{h}_{u^+} = 1$  and  $\mathbf{h}_i^T \mathbf{h}_{i^+} = 1$ , and let

TABLE II  
COMPARISON OF TIME COMPLEXITY.

Complexity/Model	DirectSpec	CL	GCL
Self-supervised	$c \mathbf{R}^+ Bd$	$c \mathbf{R}^+ ( \mathcal{U}  +  \mathcal{I} )d$ or $c \mathbf{R}^+ Bd$	$c \mathbf{R}^+  \left( \frac{L \mathbf{R}^+ }{B} +  \mathcal{U} ^2 +  \mathcal{I} ^2 \right) d$
Supervised	$c \mathbf{R}^+ d$	$2c \mathbf{R}^+ d$ or $c \mathbf{R}^+ Bd$	$2c \mathbf{R}^+ d$

$L_{cl}(u) = -\ln \frac{\exp(1/\tau)}{\sum_v \exp(\mathbf{h}_u^T \mathbf{h}_v / \tau)}$ . Then, the gradients over the parameters are calculated as follows:

$$\begin{aligned} \frac{\partial L_{cl}}{\partial \mathbf{h}_u} &= \frac{\partial L_{cl}(u)}{\partial \mathbf{h}_u} + \sum_{v \neq u} \frac{\partial L_{cl}(v)}{\partial \mathbf{h}_u} \\ &= \sum_v \frac{\exp(\mathbf{h}_u^T \mathbf{h}_v / \tau)}{\sum_k \exp(\mathbf{h}_u^T \mathbf{h}_k / \tau)} \mathbf{h}_v / \tau + \sum_v \frac{\exp(\mathbf{h}_v^T \mathbf{h}_v / \tau)}{\sum_k \exp(\mathbf{h}_v^T \mathbf{h}_k / \tau)} \mathbf{h}_v / \tau, \end{aligned} \quad (24)$$

thus the parameters are updated via SGD as:

$$\mathbf{H}_U \leftarrow \mathbf{H}_U - \alpha \cdot \left( \text{softmax}\left(\mathbf{H}_U \mathbf{H}_U^T / \tau\right) + \mathbf{S} \mathbf{D}^{-1} \right) \mathbf{H}_U, \quad (25)$$

where  $\mathbf{S} = \exp\left(\mathbf{H}_U \mathbf{H}_U^T / \tau\right)$ , and  $\mathbf{D}$  is a diagonal matrix with  $D_{uu} = \sum_v \mathbf{S}_{uv}$ ,  $\text{softmax}\left(\mathbf{H}_U \mathbf{H}_U^T / \tau\right) = \mathbf{D}^{-1} \mathbf{S}$ . Item embeddings are updated in a way similar to Equation (25). We can see that Equation (25) is the same as DirectSpec<sup>+</sup> if we ignore the term  $\mathbf{S} \mathbf{D}^{-1}$ , revealing that uniformity can alleviate collapse by indirectly rebalancing the embedding spectrum.

The superiority of DirectSpec over CL-based methods are two aspects. Firstly, CL-based methods generate and compare different node views based on data augmentation, requiring more complexity than our methods. In addition, DirectSpec is more effective tackling the embedding collapse issue as we showed that CL-based methods rebalance the embedding spectrum in a more indirect and implicit way. We will demonstrate the above two claims in Section V-B.

2) *Complexity:* We compare the complexity of DirectSpec with graph contrastive learning (GCL) and CL in Table II, where  $B$  and  $c$  denote the batch size and the required epochs, respectively. All the three methods adopt a multi-task training strategy, where the complexity comes from the supervised and self-supervised learning task (if we consider the process of spectrum balancing in DirectSpec as a self-supervised learning task). For self-supervised learning task, GCL has expensive computational cost as it generates two node views on perturbed graphs, whose time complexity is twice that of the backbone GCN (here, we use LightGCN). CL has lower time complexity than GCL as it does not exploit graph structures, and the complexity can be reduced to that of DirectSpec:  $c|\mathbf{R}^+|Bd$  if it adopts a mini-batch training [22] (the complexity in practical should be higher as we do not consider the complexity for data augmentation here). For supervised learning task, we ignore the computational cost of the encoder (*i.e.*, the complexity for generating the embeddings) as DirectSpec and CL can also be implemented on other algorithms (*e.g.*, MLP, GNN, transformer, etc.). Compared with most of the works adopting BPR or CL loss which still rely on negative samples, DirectSpec only samples the positive pairs and is equipped with a simple

TABLE III  
STATISTICS OF DATASETS.

Datasets	#User	#Item	#Interactions	Density%
CiteULike	5,551	16,981	210,537	0.223
Yelp	25,677	25,815	731,672	0.109
Gowalla	29,858	40,981	1,027,370	0.084

loss. Overall, DirectSpec shows lower time complexity over GCL and CL methods.

3) *Comparison between Embedding Collapse and Over-Smoothing*: Embedding collapse is a general issue on recommendation algorithms that can be mathematically formulated as follows:

$$\text{rank}(\mathbf{H}^{(L)}) \leq \epsilon, \quad (26)$$

where  $\mathbf{H}^{(L)}$  is the embedding when erank converges after updating  $L$  times,  $\epsilon < d$ , and a smaller  $\epsilon$  indicates a more serious collapse. On the other hand, over-smoothing only exists on GNN-based methods caused by repeating the message passing rule, which can be considered as a complete collapse issue and be formulated as Equation (26) ( $\epsilon \ll d$ ). Therefore, our proposed DirectSpec is expected to well address over-smoothing as well. Existing solutions alleviate the over-smoothing mostly by randomly dropping out the edges to perturb the spectrum [25] or balancing the contribution of different order neighborhood [26] to avoid all eigenvalues from shrinking. We can see that these methods can only slow the speed of collapse or prevent user/item representations from being the same (*i.e.*, complete collapse), while there is no guarantee that incomplete collapse can also be prevented (*i.e.*,  $d > \tau > 1$ ). We will demonstrate the effectiveness of our methods for over-smoothing in Section V-B3.

## V. EXPERIMENTS

In this section, we comprehensively evaluate our proposed methods on three public datasets. We implement DirectSpec on two popular baselines: MF and LightGCN. Particularly, we introduce data description and implementation details in Section V-A; we compare DirectSpec with other competitive baselines in terms of accuracy and efficiency in Section V-B. Finally, we conduct model analysis in Section V-C, including detailed analysis and experimental results on how DirectSpec prevents embeddings from collapsing without relying on negative samples, and how different settings of hyperparameters affect model performance.

### A. Experimental Settings

1) *Datasets*: We use the following three publicly available real-world datasets in this work, where the statistics of them are summarized in Table III.

- **CiteULike**<sup>2</sup>: This is a scholarly article recommendation dataset. Users are allowed to create their own collections of articles including abstracts, titles, and tags, etc.

<sup>2</sup><https://github.com/js05212/citeulike-a>

- **Yelp** [27]: This is a business dataset from Yelp Challenge data. The items are point of interests (POIs), users can leave reviews and ratings.
- **Gowalla** [15]: This is a check-in datasets recording which locations users have visited.

Since we focus on CF for implicit feedbacks, we remove auxiliary information such as reviews, tags, geological and item information, etc, and transform explicit ratings to 0-1 implicit feedbacks.

2) *Evaluation Metrics*: We adopt two widely used evaluation metrics for personalized rankings: Recall and normalized discounted cumulative gain (nDCG) [28] to evaluate model performance. The recommendation list is generated by ranking unobserved items and truncating at position  $k$ . Recall measures the ratio of the relevant items in the recommendation list to all relevant items in test sets, while nDCG takes the rank into consideration by assigning higher scores to the relevant items ranked higher. We use 80% of the interactions for training and randomly select 10% from the training set as validation set for hyper-parameter tuning, the rest 20% data is used for test sets; we report the average accuracy on test sets.

3) *Baselines*: We compare DirectSpec with the following competitive baselines:

- BPR [12]: This is a stable and classic MF-based method, exploiting a Bayesian personalized ranking loss for personalized rankings.
- CL-Rec [22]: This is a CL-based method. Since there are no item features on the datasets used in this work, we remove data augmentation and use BPR as the main loss to better compare with our methods.
- ENMF [29]: This is a neural recommendation model performing whole-data-based learning without sampling. We choose user-based ENMF as the baseline.
- CCL [13]: The proposed cosine contrastive loss (CCL) maximizes the similarity between positive pairs and minimizes the similarity of negative pairs below the margin  $m$ . After parameter tuning, we set  $\mathcal{N} = 1000$ ,  $w = 300$  on all datasets,  $m = 0.1, 0.3$ , and  $0.3$  on CiteULike, Yelp, and Gowalla, respectively, and we choose MF as the encoder.
- DirectAU [23]: This method directly optimizes alignment and uniformity and shows superior performance. Following the original paper, we choose MF and LightGCN as the encoder, and set  $\gamma = 5.0, 0.5$ , and  $1.5$  on CiteULike, Yelp, and Gowalla, respectively.
- LightGCN [14]: This is a linear GNN method that only keeps neighborhood aggregation for recommendation. We employ a three-layer architecture as our baseline.
- SGL-ED [21]: This model explores self-supervised learning by maximizing the agreements of multiple views from the same node, where the node views are generated by adding noise such as randomly removing the edges or nodes on the original graph. We set  $\tau = 0.2$ ,  $\lambda_1 = 0.1$ ,  $p = 0.1$ , and use a three-layer architecture.
- LightGCL [30]: This is a simple yet effective graph contrastive learning method injecting global collaborative relations via singular value decomposition.
- GDE [31]: This method only keeps a very few graph features for recommendation without stacking layers, showing



TABLE IV  
PERFORMANCE COMPARISON. THE BEST BASELINE IS UNDERLINED. “\*” INDICATES STATISTICAL SIGNIFICANCE AT  $p < 0.01$  FOR A ONE-TAILED T-TEST.

	CiteULike				Yelp				Gowalla			
	nDCG@ $k$		Recall@ $k$		nDCG@ $k$		Recall@ $k$		nDCG@ $k$		Recall@ $k$	
	$k=10$	$k=20$	$k=10$	$k=20$	$k=10$	$k=20$	$k=10$	$k=20$	$k=10$	$k=20$	$k=10$	$k=20$
BPR	0.1620	0.1773	0.1778	0.2190	0.0487	0.0583	0.0607	0.0869	0.1164	0.1255	0.1186	0.1483
CL-REC	0.1523	0.1662	0.1671	0.2069	0.0476	0.0566	0.0588	0.0833	0.1116	0.1198	0.1123	0.1401
CCL(MF)	0.1545	0.1642	0.1716	0.1996	0.0509	0.0593	0.0617	0.0846	0.1269	0.1349	0.1295	0.1573
EMNF-U	0.1335	0.1601	0.1556	0.2193	0.0665	0.0811	0.0786	0.1167	0.1166	0.1286	0.1173	0.1528
DirectAU(MF)	<u>0.2102</u>	<u>0.2252</u>	<u>0.2260</u>	<u>0.2693</u>	<u>0.0721</u>	<u>0.0848</u>	<u>0.0872</u>	<u>0.1219</u>	0.1286	0.1402	0.1349	0.1710
DirectAU(GCN)	0.1926	0.2109	0.2116	0.2604	0.0695	0.0819	0.1194	0.1194	0.1298	0.1409	0.1363	0.1711
LightGCN	0.1610	0.1781	0.1771	0.2190	0.0572	0.0690	0.0721	0.1045	0.0987	0.1098	0.1074	0.1399
SGL-ED	0.1890	0.2065	0.2117	0.2588	0.0676	0.0794	0.0837	0.1166	0.1343	0.1462	0.1417	0.1779
LightGCL	0.2096	0.2238	0.2214	0.2638	0.0673	0.0790	0.0836	0.1151	<u>0.1368</u>	<u>0.1482</u>	<u>0.1436</u>	<u>0.1801</u>
GDE	0.1890	0.2061	0.2055	0.2528	0.0653	0.0771	0.0805	0.1129	0.1261	0.1367	0.1313	0.1656
LogDet	0.1403	0.1579	0.1548	0.2034	0.0711	0.0833	0.0863	0.1203	0.1179	0.1272	0.1203	0.1151
DirectSpec(MF)	0.1688	0.1849	0.1827	0.2270	0.0689	0.0804	0.0839	0.1156	0.1133	0.1225	0.1183	0.1480
DirectSpec(GCN)	0.1693	0.1863	0.1875	0.2334	0.0712	0.0832	0.0861	0.1192	0.1160	0.1251	0.1191	0.1490
DirectSpec+(MF)	<b>0.2197*</b>	<b>0.2354*</b>	<b>0.2352*</b>	<b>0.2818*</b>	0.0743	0.0864	0.0909	0.1249	0.1389	0.1509	0.1447	<b>0.1829*</b>
DirectSpec+(GCN)	0.2038	0.2213	0.2213	0.2704	<b>0.0745*</b>	<b>0.0868*</b>	<b>0.0909*</b>	<b>0.1252*</b>	<b>0.1400*</b>	<b>0.1513*</b>	<b>0.1453*</b>	0.1819

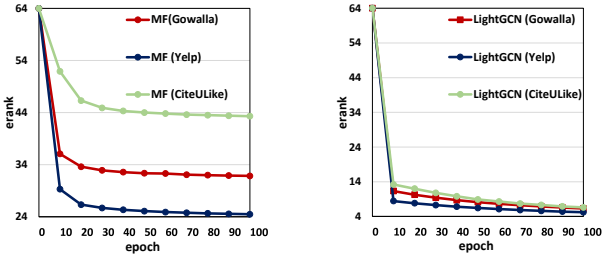


Fig. 5. The extent of collapse on three datasets.

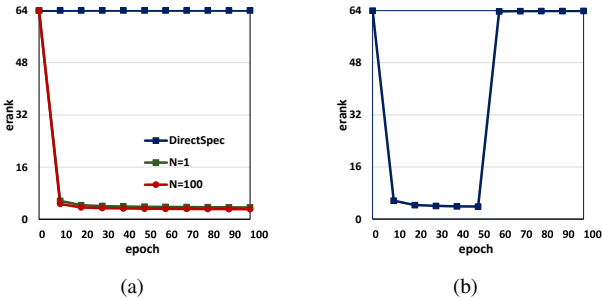


Fig. 6. All models are optimized without using observed interactions on Yelp. We show how erank changes on DirectSpec (MF) and MF (BCE) where  $N$  is the negative sampling ratio in (a). We use BCE (MF) for the first 50 epochs and DirectSpec for the last 50 epochs in (b).

less complexity and higher efficiency than conventional GCN-based methods.

- LogDet [32]: This is a decorrelation-enhanced method to mitigate the dimensional collapse of graph collaborative filtering.

4) *Implementation Details*: We implemented our DirectSpec based on PyTorch and the code is released publicly<sup>3</sup>. SGD is adopted as the optimizer for all models, the embedding size  $d$  is set to 64, the regularization rate is set to 0.01 on all datasets, the learning rate is tuned amongst  $\{0.001, 0.005, 0.01, \dots\}$ ; without specification, the model pa-

<sup>3</sup><https://github.com/tanatosuu/directspec>

TABLE V  
TRAINING TIME (SECONDS) PER EPOCH.

Model/Data	Citeulike	Yelp	Gowalla
BPR	2.37	8.53	13.28
DirectSpec+(MF)	3.78 (1.59x)	13.15 (1.54x)	19.10 (1.44x)
LightGCN	8.78	43.18	79.79
DirectSpec+(GCN)	9.49 (1.08x)	45.70 (1.06x)	81.20 (1.02x)
SGL-ED(GCN)	22.20 (2.53x)	182.54 (4.23x)	401.96 (5.04x)
LightGCL(GCN)	11.59 (1.32x)	51.38 (1.19x)	92.56 (1.16x)

rameters are initialized with Xavier Initialization [33]; the batch size is set to 256. We report other hyperparameter settings in the next subsection.

## B. Comparison

1) *Performance*: We report overall performance in Table IV, and observe the followings:

- Overall, GCN-based methods show better performance on sparse data (Yelp and Gowalla) than dense data (CiteULike). For instance, DirectSpec+(GCN) achieves better and worse than DirectSpec+(MF) on Gowalla and CiteULike, respectively, and their performance is close on Yelp. LightGCN underperforms BPR on CiteULike and Gowalla, which might be attributed to the slow convergence that has been reported in the original paper. Among baselines, DirectAU achieves the best on CiteULike and Yelp, while LightGCL outperforms other baselines on Gowalla. Our proposed DirectSpec+ implemented on both LightGCN and MF consistently show improvements over all baselines.
- CL-Rec is even inferior to BPR, indicating that it is hard for traditional CF task without any side information to benefit from CL. In the meanwhile, the GCL-based method (SGL-ED and LightGCL) works much better as we can exploit the graph structure containing rich topological information as the input, as opposed to traditional CF task that only uses user/item ID as input.
- DirectAU directly regulating the uniformity shows relatively superior performance. Inspired by [20], it adopts a Radial Basis Function kernel which shares a similar form to the

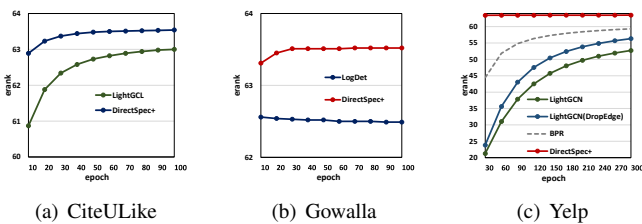


Fig. 7. Erank comparison among several methods.

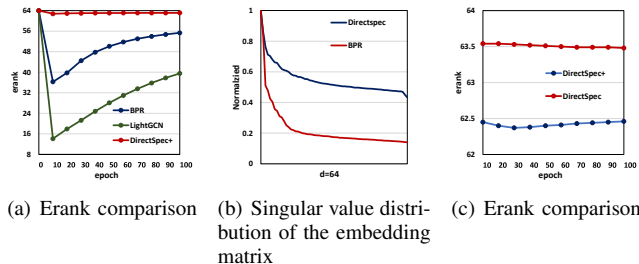


Fig. 8. How DirectSpec prevents collapse (on Yelp).

uniformity loss. Since we have shown that the uniformity loss can tackle embedding collapse by indirectly balancing the spectrum distribution in Section IV-D1, the effectiveness of DirectAU demonstrates our previous analysis.

- Since our methods are implemented on MF and LightGCN, the effectiveness of our methods can be further demonstrated by directly comparing with them. DirectSpec(MF) and DirectSpec<sup>+</sup>(MF) outperform BPR by 14.3% and 35.8%, on average in terms of nDCG@10, respectively. In the meanwhile, the improvement of DirectSpec(GCN) and DirectSpec<sup>+</sup>(GCN) over LightGCN is 15.7% and 32.9% on average in terms of nDCG@10, respectively.
- Overall, the improvement of DirectSpec over MF and LightGCN is  $\text{Yelp} > \text{Gowalla} > \text{CiteULike}$  (33.0%, 7.4%, and 4.7% on average in terms of nDCG@10, respectively). Figure 5 compares the extent of collapse on three datasets using MF and LightGCN (with only positive samples). We can observe that Yelp suffers more from the collapse while CiteULike suffers less, which is consistent with the improvement of DirectSpec. This observation reveals that the dataset suffering more from collapse tends to benefit more from DirectSpec.
- DirectSpec<sup>+</sup> shows significant improvement over DirectSpec across all datasets. As introduced in Section IV-C DirectSpec<sup>+</sup> is more effective tackling embedding collapse than DirectSpec by effectively penalizing the hard negative samples with user/item pairs highly correlated. The superior performance demonstrates its effectiveness.

2) *Efficiency*: We report the training time per epoch of BPR, LightGCN, and DirectSpec<sup>+</sup> (MF and GCN) in Table V. The experiments are all conducted on Intel(R) Core(TM) i9-10980XE CPU and NVIDIA RTX A6000 GPU. We first compare BPR and DirectSpec<sup>+</sup>(MF), and observe that it takes roughly 0.5x additional running time, which is acceptable considering the significant improvement. DirectSpec<sup>+</sup>(GCN) almost shows no additional running time over LightGCN, due

to the reason that the complexity of DirectSpec<sup>+</sup> is mainly determined by the batch size rather than the size of users and items. Since LightGCN has a higher complexity than BPR, the proportion of DirectSpec<sup>+</sup>(LightGCN)’s running time to that of LightGCN is much smaller than the proportion of DirectSpec<sup>+</sup>(MF)’s running time to that of BPR. This finding can explain another observation that the additional time is smaller on larger datasets (*i.e.*,  $\text{Gowalla} < \text{Yelp} < \text{CiteULike}$ ). The complexity of DirectSpec<sup>+</sup> is unchanged while LightGCN and BPR accordingly take more running time on larger datasets, thus the proportion of DirectSpec<sup>+</sup>’s running time to that of LightGCN/BPR becomes smaller. Meanwhile, SGL-ED is more computationally expensive on larger datasets, and DirectSpec<sup>+</sup>(LightGCN) is more efficient than it with more significant improvement over LightGCN.

### 3) Comparison w.r.t Effective Rank: Negative Sampling.

The results in Table IV demonstrates the superiority of DirectSpec over negative sampling based methods including BPR and CCL in terms of performance. Furthermore, we compare how these two methods alleviate collapse issue by optimizing them solely based on unobserved interactions. In Figure 6 (a), we observe that the erank of MF (BCE) consistently drops without optimization on the observed interactions, resulting in a complete collapse, and the erank drops more quickly as increasing the negative sampling ratios, whereas the erank of DirectSpec remains unchanged throughout the training. This observation indicates that there exists a dynamic balance between optimization on observed and unobserved interactions, the lack of either of them cannot prevent the embeddings from collapsing. Furthermore, since negative sampling is equivalent to a high pass filter, it can only alleviate the collapse caused by low pass filters (*e.g.*, optimization on observed interactions), while DirectSpec is equivalent to an all pass filter that can tackle the collapse under any situations. Figure 6 (b) demonstrates that DirectSpec can recover the embeddings from collapsing caused by negative sampling.

**LightGCL** is an effective and efficient CL-based method with the design of uniformity helping alleviate the collapse issue. As shown in Figure 7 (a), the erank of LightGCL is lower than DirectSpec<sup>+</sup> at the beginning, gradually increases as training proceeds and converges to a value smaller than the erank of DirectSpec<sup>+</sup>, demonstrating the superiority of DirectSpec tackling the collapse issue over LightGCL, explaining why it shows better performance.

**LogDet** is an enhanced method improving based on uniformity-based methods. As shown in Figure 7 (b), the erank of LogDet remains stable and closer to  $d$  than LightGCL, showing a better ability tackling collapse issue than uniformity-based methods. Meanwhile, it still exhibits a lower erank than our proposed DirectSpec<sup>+</sup> throughout the training.

**Solutions to Over-Smoothing**. As shown in Section IV, embedding collapse is attributed to the optimization part and over-smoothing (for GNN-based methods). In this subsection, we investigate (1) if the solutions to over-smoothing can also well address the collapse issue and (2) Do DirectSpec show superiority over them in addressing the over-smoothing. To this end, we compare DropEdge [25] (implemented on LightGCN), a solution to over-smoothing, LightGCN (suffer from

both (1) and (2)), and BPR (suffer from (1)) with DirectSpec<sup>+</sup>. We report how their eranks change throughout the training in Figure 7 (c). We can see the erank of DropEdge is higher than LightGCN while lower than BPR during the training, indicating that the solution to over-smoothing can only alleviate (2) while fails to tackle (1), the main cause of collapse issue analyzed in this work. Furthermore, DirectSpec<sup>+</sup> shows a higher and more stable erank than DropEdge, demonstrating a better capability in addressing over-smoothing than DropEdge.

### C. Model Analysis

1) *Can DirectSpec Prevent Collapse?:* In Figure 8 (a), we report how the erank changes as training proceeds on BPR, LightGCN, and DirectSpec<sup>+</sup>(MF). For BPR and LightGCN, the erank plunges significantly in the first place, then increases slowly and tends to converge to a value smaller than  $d$ , resulting in an incomplete embedding collapse. While the erank of DirectSpec<sup>+</sup>(MF) is close to  $d$  at the beginning of training and remains almost unchanged throughout the training. Figure 8 (b) illustrates the normalized singular value distribution of the embedding matrix when the accuracy of BPR and DirectSpec<sup>+</sup>(MF) is maximized. We can see that most singular values of BPR’s embeddings are less than 0.2, barely contributing to the representations; while DirectSpec<sup>+</sup>(MF)’s singular values are mostly larger than 0.5, indicating that the representations are contributed by more dimensions. One may raise a concern, that DirectSpec still suffers from embedding collapse as the erank is still slightly smaller than  $d$  ( $d = 64 > \text{erank}(\mathbf{H}) > 62$  in our experiments) when the accuracy is maximized. As shown in Section IV-B, the goal of DirectSpec is equivalent to decorrelating users and items, while it is obvious that not all users/items are irrelevant, considering the relations of observed interactions (*e.g.*, users share similar/opposite interests are positively/negatively related; items that are interacted by similar users or users that have opposite interests are also positively or negatively correlated, respectively). Thus, a higher erank does not necessarily lead to a better accuracy. From a spectral perspective, all dimensions are not completely equally important to users/item. Some dimensions might contain more important information while others contain less. In other words, the goal of DirectSpec is to assure that all dimensions literally contribute to the representations, as opposed to the representations of BPR or LightGCN that are only predominantly distributed along a few dimensions. In Figure 8 (c), DirectSpec seems to show a better ability of balancing spectrum as it has a higher erank, while it shows inferior performance to DirectSpec<sup>+</sup>. As shown in Equation (15), all samples are decorrelated with the same pace on DirectSpec, thus the similar or dissimilar (*i.e.*, sharing opposite interests) users/items that should be correlated to some extent are also perfectly orthogonalized, leading to underfitting.

2) *Adaptive Temperature Design:* We first compare the dynamic and static designs proposed in Section IV-C, and report the results in Table VI. We observe that the static design outperforms the dynamic design by a large margin on all datasets, and the reason might be attributed to the data

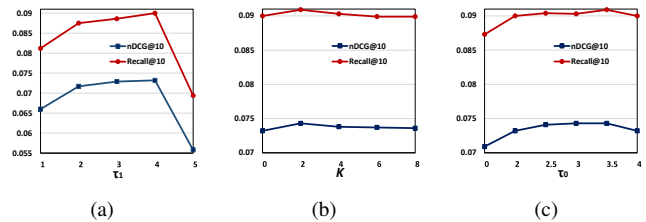


Fig. 9. (a) shows how the accuracy changes with  $\tau_1$ , (b) displays the sensitivity of  $k$ , and (c) illustrates how the accuracy changes with  $\tau_0$  on Yelp.

TABLE VI  
COMPARISON BETWEEN STATIC AND DYNAMIC TEMPERATURE DESIGN.

	Citeulike		Yelp		Gowalla	
	nDCG@10	Recall@10	nDCG@10	Recall@10	nDCG@10	Recall@10
Static (i)	0.2197	0.2352	0.0743	0.0909	0.1389	0.1447
Dynamic (ii)	0.1593	0.1693	0.0485	0.0611	0.1126	0.1144

scarcity on CF task, making the algorithm difficult to learn the inherent user/item relations from the interactions data in a dynamic way. Therefore, DirectSpec<sup>+</sup> is implemented with a static temperature design, which avoids bringing additional complexity. We first tune  $\tau_1$  by fixing  $\tau_0 = \tau_1$  and report how the accuracy changes with  $\tau_1$  in Figure 9 (a) and (b). The accuracy first increases and then drops as  $\tau_1$  increases, which is maximized at  $\tau_1 = 4$  on Yelp.  $\tau_1$  controls the strength of penalties on highly correlated unobserved samples (*i.e.*, hard negatives), the samples that are not highly correlated tend to be ignored when  $\tau_1$  is set too large, while a too small  $\tau_1$  fails to optimize the highly correlated samples in an effective way. On the other hand, among all unobserved interactions, some are correlated to some extent that should be decorrelated with a slower pace which we use another hyperparameter  $\tau_0$  to control. In Figure 9 (b), we observe that optimizing the user/item pairs whose graph distance are  $K = 2$  with a slower pace  $\tau_0$  results in a better accuracy, and the accuracy drops after introducing the pairs farther away (*i.e.*,  $K > 2$ ) as they are too far away on the graph that should be considered irrelevant. In Figure 9 (c), DirectSpec<sup>+</sup> achieves the best performance at  $\tau_0 = 3.5$  which is slightly smaller than  $\tau_1 = 4$  on Yelp (see Figure 9 (a)), and further decreasing  $\tau_0 = 3.5$  leads to a worse performance. This finding indicates that the correlation between the pairs that are close on the graph are still significantly smaller than the observed interactions.

3) *Impact of  $\alpha$ :* According to Equation (13),  $\alpha$  controls the extent of spectrum balancing. A larger (smaller)  $\alpha$  implies that large singular values are multiplied by smaller (larger) weights, leading to a more (less) uniform spectrum distribution. Proposition 1 does not hold when  $\alpha$  is too large:  $1 - \alpha\sigma_1^2 < 0$  (with  $L = 1$ ). Since it takes additional time to calculate  $\sigma_1$  during each training, we use the grid search for optimal  $\alpha$ . As shown in Figure 10 (a) and (b), both of the accuracy and erank first increase and then drop, showing a similar trend. Specifically, the speed of collapse tends to outrun the speed of spectrum balancing when  $\alpha$  is small, and the drop in erank as increasing  $\alpha$  demonstrates our analysis in Section IV-A that a large  $\alpha$  instead results in a sharp distribution. In addition,

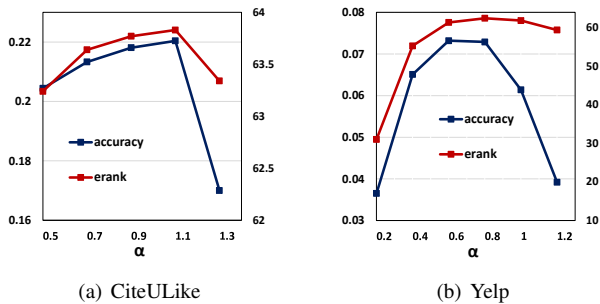


Fig. 10. Impact of  $\alpha$  on accuracy (nDCG@10) and erank.

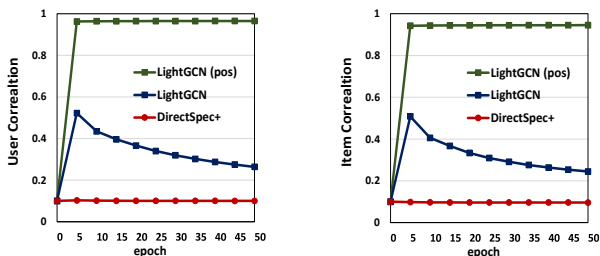


Fig. 11. Correlations of users (left) and items (right) during the training.

the best performance is achieved at  $\alpha = 1.1$  on CiteULike and  $\alpha = 0.6$  on Yelp, and the erank and accuracy are more sensitive when  $\alpha$  is small on Yelp, which might be related to the fact that Yelp suffers more from the collapse issue than other datasets.

4) *User/Item Correlation*: As analyzed in Section IV-C, the user/item correlation can reflect the extent of embedding collapse, and the correlation here is measured by Equation (14). As shown in Figure 11, the correlation is low before training, while users/items become highly correlated immediately after training starts on LightGCN(pos) which only optimizes positive (*i.e.*, observed) pairs, causing user and items to have similar representations and resulting in a complete collapse. For LightGCN using BPR loss, the correlation first immediately increases and then gradually drops, whereas the correlation keeps low throughout the training on DirectSpec<sup>+</sup>, demonstrating its effectiveness to tackle embedding collapse. On the other hand, correlation can also measure the extent of over-smoothing that a higher value indicates more similar representations for GNN-based methods. Since it has been shown that LightGCN helps alleviate the over-smoothing, the lower correlation of DirectSpec<sup>+</sup> than LightGCN also indicates the superiority of our proposed method addressing over-smoothing. We also notice that the correlation did not converges to 0, due to the reason that  $\mathbf{H}_U \mathbf{H}_U^T$  and  $\mathbf{H}_I \mathbf{H}_I^T$  are full rank matrices when they are optimized to identity matrices (*i.e.*, completely decorrelated) according to Equation (14), while the embedding matrix is merely a low-rank approximation:  $d \ll \min(|\mathcal{U}|, |\mathcal{I}|)$ , thus the correlation would not converge to 0 unless  $d \geq \max(|\mathcal{U}|, |\mathcal{I}|)$ .

## VI. RELATED WORK

### A. Collaborative Filtering

Collaborative Filtering (CF), a fundamental task for recommender systems, makes predictions based on user’s past behaviours. Early CF methods exploit users that share similar interests or items that tend to be interacted by similar users to infer user preference [34]. Nowadays, model-based methods are prevalent in CF and recommender systems. The core idea is to map the high dimensional sparse recommendation data to a low-dimensional space, where users and items are characterized as learnable vectors and are optimized based on observed interactions [4]. With the development of computer hardware and communication network, more information can be collected to analyze user behaviour with advanced algorithms. Besides user-item interactions, side information such as social relations [3], reviews [35], geological information [36], [37], and so on can help the algorithms better understand user taste and preference. On another line, early simple CF methods [4], [38] are replaced by more powerful algorithms such as neural network [5], [39], attention mechanism [6], [40], transformer [8], etc. Recently, graph neural network (GNN) has also shown tremendous success in recommender systems [11], [15], [25]. By representing interactions as a bipartite graph, the core idea of GNN is to exploit higher-order neighbor connections to facilitate user/item representations [18]. However, it has been reported that multi-layer GNNs suffer from an over-smoothing issue that causes user/item representations to be indistinguishable [19], [31]. We showed that an embedding collapse issue resembling the over-smoothing exists on recommendation algorithms in general, and our proposed approach has also been shown effective tackling over-smoothing.

### B. Collapse in Representation Learning

Representation learning has attracted tremendous attention in various research fields [41], [42], the goal of which is to represent data in an effective and efficient way to make it easier to extract useful information when building predictors. However, it has also been shown that the model tends to collapse where all inputs are mapped to the same constant vector, when only optimizing the model based on the positive pairs [43]. This issue can be well alleviated by self-supervised learning and contrastive learning by exploiting negative samples in an effective way [44]. Due to the heavy computation cost, some research effort has been made to simplify the algorithms without explicitly sampling negative data [43], [45], [46]. Unfortunately, subsequent works show that a dimensional collapse cannot be ignored where the embedding vectors end up spanning a lower dimensional subspace of the whole embedding space [47], [48]. The collapse issue in representation learning shares similarities to some issues such as over-smoothing in GNN [19], which inspires some researchers to tackle issues in GNN [49], [50].

Inspired by the aforementioned works tackling collapse in representation learning, we reviewed existing recommendation methods, and showed that they suffer from a collapse issue as well. Particularly, the representations tend to collapse to a constant vector when only optimization observed interactions,

and an incomplete collapse still exists despite introducing negative samples [5], [12] where the representations are predominantly distributed in certain dimensions. We showed that CL-based methods help tackle this issue to some extent due to the uniformity loss which implicitly balances the embedding spectrum [21], [23], [30]. We address this issue from a spectral perspective by directly balancing the embedding spectrum, which has been demonstrated more effective than existing works. Lastly, we notice a recent work [32] also points out a dimensional collapse issue sharing similarity with our work, while we demonstrated the superiority over it in terms of performance and the effectiveness tackling the collapse issue.

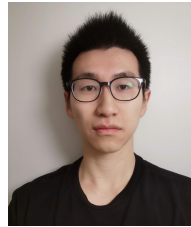
## VII. CONCLUSION

In this work, we showed that existing CF methods mostly suffer from an embedding collapse issue. Particularly, optimization solely on the observed interactions causes the representations to collapse to a constant vector, while negative sampling that can decelerate the collapse by balancing the embedding spectrum still results in an incomplete collapse. To tackle this issue, we proposed a DirectSpec which acts as an all pass filter to directly balances the spectrum distribution to ensure that all dimensions can contribute to the user/item embeddings as equally as possible. We conducted comprehensive analysis on DirectSpec from a decorrelation perspective and further proposed an enhanced variant DirectSpec<sup>+</sup> to efficiently penalize irrelevant samples with self-paced gradients. In addition, we shed light on the close connection between DirectSpec<sup>+</sup> and contrastive learning, that uniformity, a key design contributing to recommendation, can alleviate collapse issue by indirectly balancing spectrum distribution, that can be considered as a special case of DirectSpec<sup>+</sup>. Finally, extensive experiments on three publicly available datasets demonstrated the effectiveness and efficiency of our proposed methods.

## REFERENCES

- [1] J. Wang, P. Huang, H. Zhao, Z. Zhang, B. Zhao, and D. L. Lee, "Billion-scale commodity embedding for e-commerce recommendation in alibaba," in *Proceedings of the 24th ACM SIGKDD International Conference on Knowledge Discovery & Data Mining (KDD'18)*, 2018, pp. 839–848.
- [2] S. Liu, Z. Chen, H. Liu, and X. Hu, "User-video co-attention network for personalized micro-video recommendation," in *Proceedings of the 28th international conference on World Wide Web (WWW'19)*, 2019, pp. 3020–3026.
- [3] M. Jiang, P. Cui, R. Liu, Q. Yang, F. Wang, W. Zhu, and S. Yang, "Social contextual recommendation," in *Proceedings of the 21st ACM International Conference on Information and Knowledge Management (CIKM'12)*, 2012, pp. 45–54.
- [4] Y. Koren, R. Bell, and C. Volinsky, "Matrix factorization techniques for recommender systems," *Computer*, no. 8, pp. 30–37, 2009.
- [5] X. He, L. Liao, H. Zhang, L. Nie, X. Hu, and T.-S. Chua, "Neural collaborative filtering," in *Proceedings of the 26th International Conference on World Wide Web (WWW'17)*, 2017, pp. 173–182.
- [6] W.-C. Kang and J. McAuley, "Self-attentive sequential recommendation," in *2018 IEEE International Conference on Data Mining (ICDM'18)*, 2018, pp. 197–206.
- [7] G. Zheng, F. Zhang, Z. Zheng, Y. Xiang, N. J. Yuan, X. Xie, and Z. Li, "Dm: A deep reinforcement learning framework for news recommendation," in *Proceedings of the 27th International Conference on World Wide Web (WWW'18)*, 2018, pp. 167–176.
- [8] F. Sun, J. Liu, J. Wu, C. Pei, X. Lin, W. Ou, and P. Jiang, "Bert4rec: Sequential recommendation with bidirectional encoder representations from transformer," in *Proceedings of the 28th ACM International Conference on Information and Knowledge Management (CIKM'19)*, 2019, pp. 1441–1450.
- [9] W. Wang, Y. Xu, F. Feng, X. Lin, X. He, and T.-S. Chua, "Diffusion recommender model," in *Proceedings of the 46th International ACM SIGIR Conference on Research and Development in Information Retrieval (SIGIR'23)*, 2023, p. 832–841.
- [10] R. Ying, R. He, K. Chen, P. Eksombatchai, W. L. Hamilton, and J. Leskovec, "Graph convolutional neural networks for web-scale recommender systems," in *Proceedings of the 24th ACM SIGKDD International Conference on Knowledge Discovery & Data Mining (KDD'18)*, 2018, pp. 974–983.
- [11] S. Peng, K. Sugiyama, and T. Mine, "Svd-gcn: A simplified graph convolution paradigm for recommendation," in *Proceedings of the 31st ACM International Conference on Information & Knowledge Management (CIKM'22)*, 2022, pp. 1625–1634.
- [12] S. Rendle, C. Freudenthaler, Z. Gantner, and L. Schmidt-Thieme, "Bpr: Bayesian personalized ranking from implicit feedback," in *Proceedings of the 25th Conference on Uncertainty in Artificial Intelligence (UAI'09)*, 2009, pp. 452–461.
- [13] K. Mao, J. Zhu, J. Wang, Q. Dai, Z. Dong, X. Xiao, and X. He, "Simplex: A simple and strong baseline for collaborative filtering," in *Proceedings of the 30th ACM International Conference on Information & Knowledge Management (CIKM'21)*, 2021, pp. 1243–1252.
- [14] X. He, K. Deng, X. Wang, Y. Li, Y. Zhang, and M. Wang, "Lightgcn: Simplifying and powering graph convolution network for recommendation," in *Proceedings of the 43rd International ACM SIGIR Conference on Research and Development in Information Retrieval (SIGIR'20)*, 2020, pp. 639–648.
- [15] X. Wang, X. He, M. Wang, F. Feng, and T.-S. Chua, "Neural graph collaborative filtering," in *Proceedings of the 42nd international ACM SIGIR conference on Research and development in Information Retrieval (SIGIR'19)*, 2019, pp. 165–174.
- [16] O. Roy and M. Vetterli, "The effective rank: A measure of effective dimensionality," in *2007 15th European Signal Processing Conference*, 2007, pp. 606–610.
- [17] A. Sandryhaila and J. M. Moura, "Discrete signal processing on graphs: Frequency analysis," *IEEE Transactions on Signal Processing*, vol. 62, no. 12, pp. 3042–3054, 2014.
- [18] T. N. Kipf and M. Welling, "Semi-supervised classification with graph convolutional networks," in *Proceedings of the 5th International Conference on Learning Representations (ICLR'17)*, 2017.
- [19] Q. Li, Z. Han, and X.-M. Wu, "Deeper insights into graph convolutional networks for semi-supervised learning," in *Proceedings of the 32nd AAAI Conference on Artificial Intelligence (AAAI-18)*, 2018, pp. 3538–3545.
- [20] T. Wang and P. Isola, "Understanding contrastive representation learning through alignment and uniformity on the hypersphere," in *International Conference on Machine Learning (ICML'20)*, 2020, pp. 9929–9939.
- [21] J. Wu, X. Wang, F. Feng, X. He, L. Chen, J. Lian, and X. Xie, "Self-supervised graph learning for recommendation," in *Proceedings of the 44th International ACM SIGIR Conference on Research and Development in Information Retrieval (SIGIR'21)*, 2021, pp. 726–735.
- [22] T. Yao, X. Yi, D. Z. Cheng, F. Yu, T. Chen, A. Menon, L. Hong, E. H. Chi, S. Tjoa, J. J. Kang, and E. Ettinger, "Self-supervised learning for large-scale item recommendations," in *Proceedings of the 30th ACM International Conference on Information & Knowledge Management (CIKM'21)*, 2021, p. 4321–4330.
- [23] C. Wang, Y. Yu, W. Ma, M. Zhang, C. Chen, Y. Liu, and S. Ma, "Towards representation alignment and uniformity in collaborative filtering," in *Proceedings of the 28th ACM SIGKDD Conference on Knowledge Discovery and Data Mining (KDD'22)*, 2022, pp. 1816–1825.
- [24] J. Yu, H. Yin, X. Xia, T. Chen, L. Cui, and Q. V. H. Nguyen, "Are graph augmentations necessary? simple graph contrastive learning for recommendation," in *Proceedings of the 45th International ACM SIGIR Conference on Research and Development in Information Retrieval (SIGIR'22)*, 2022, pp. 1294–1303.
- [25] Y. Rong, W. Huang, T. Xu, and J. Huang, "Dropege: Towards deep graph convolutional networks on node classification," in *Proceedings of the 8th International Conference on Learning Representations (ICLR'20)*, 2020.
- [26] J. Gasteiger, A. Bojchevski, and S. Günnemann, "Predict then propagate: Graph neural networks meet personalized pagerank," in *Proceedings of the 7th International Conference on Learning Representations (ICLR'19)*, 2019.

- [27] X. He, H. Zhang, M.-Y. Kan, and T.-S. Chua, “Fast matrix factorization for online recommendation with implicit feedback,” in *Proceedings of the 39th international ACM SIGIR conference on Research and development in Information Retrieval (SIGIR’16)*, 2016, pp. 549–558.
- [28] K. Järvelin and J. Kekäläinen, “Cumulated gain-based evaluation of ir techniques,” *ACM Transactions on Information Systems (TOIS)*, vol. 20, no. 4, pp. 422–446, 2002.
- [29] C. Chen, M. Zhang, Y. Zhang, Y. Liu, and S. Ma, “Efficient neural matrix factorization without sampling for recommendation,” *ACM Transactions on Information Systems (TOIS)*, vol. 38, no. 2, pp. 1–28, 2020.
- [30] X. Cai, C. Huang, L. Xia, and X. Ren, “Lightgcl: Simple yet effective graph contrastive learning for recommendation,” in *The 11th International Conference on Learning Representations (ICLR’23)*, 2023.
- [31] S. Peng, K. Sugiyama, and T. Mine, “Less is more: Reweighting important spectral graph features for recommendation,” in *Proceedings of the 45th International ACM SIGIR conference on Research and Development in Information Retrieval (SIGIR’22)*, 2022, p. 1273–1282.
- [32] Y. Zhang, H. Zhu, Z. Song, P. Koniusz, I. King *et al.*, “Mitigating the popularity bias of graph collaborative filtering: A dimensional collapse perspective,” vol. 36, pp. 67 533–67 550, 2023.
- [33] X. Glorot and Y. Bengio, “Understanding the difficulty of training deep feedforward neural networks,” in *Proceedings of the 13th International Conference on Artificial Intelligence and Statistics (AISTATS’10)*, 2010, pp. 249–256.
- [34] B. Sarwar, G. Karypis, J. Konstan, and J. Riedl, “Item-based collaborative filtering recommendation algorithms,” in *Proceedings of the 10th International Conference on World Wide Web (WWW’01)*, 2001, pp. 285–295.
- [35] Y. Bao, H. Fang, and J. Zhang, “Topicmf: Simultaneously exploiting ratings and reviews for recommendation,” in *Proceedings of the 31st AAAI Conference on Artificial Intelligence (AAAI-14)*, 2014, pp. 2–8.
- [36] D. Lian, C. Zhao, X. Xie, G. Sun, E. Chen, and Y. Rui, “Geomf: Joint geographical modeling and matrix factorization for point-of-interest recommendation,” in *Proceedings of the 20th ACM SIGKDD International Conference on Knowledge Discovery and Data Mining (KDD’14)*, 2014, p. 831–840.
- [37] S. Peng, X. Xie, T. Mine, and C. Su, “Vector representation based model considering randomness of user mobility for predicting potential users,” in *Proceedings of the 21st International Conference on the Principles and Practice of Multi-Agent Systems (PRIMA’18)*, 2018, pp. 70–85.
- [38] X. Ning and G. Karypis, “Slim: Sparse linear methods for top-n recommender systems,” in *Proceedings of the 11th International Conference on Data Mining (ICDM’11)*, 2011, pp. 497–506.
- [39] S. Sedhain, A. K. Menon, S. Sanner, and L. Xie, “Autorec: Autoencoders meet collaborative filtering,” in *Proceedings of the 24th international conference on World Wide Web (WWW’15)*, 2015, pp. 111–112.
- [40] J. Chen, H. Zhang, X. He, L. Nie, W. Liu, and T.-S. Chua, “Attentive collaborative filtering: Multimedia recommendation with item- and component-level attention,” in *Proceedings of the 40th International ACM SIGIR conference on Research and Development in Information Retrieval (SIGIR’17)*, 2017, pp. 335–344.
- [41] T. Mikolov, K. Chen, G. Corrado, and J. Dean, “Efficient estimation of word representations in vector space,” in *Proceedings of the 1st International Conference on Learning Representations (ICLR’13)*, 2013.
- [42] R. D. Hjelm, A. Fedorov, S. Lavoie-Marchildon, K. Grewal, P. Bachman, A. Trischler, and Y. Bengio, “Learning deep representations by mutual information estimation and maximization,” in *Proceedings of the 7th International Conference on Learning Representations (ICLR’19)*, 2019.
- [43] X. Chen and K. He, “Exploring simple siamese representation learning,” in *Proceedings of the IEEE/CVF Conference on Computer Vision and Pattern Recognition (CVPR’21)*, 2021, pp. 15 750–15 758.
- [44] T. Chen, S. Kornblith, M. Norouzi, and G. Hinton, “A simple framework for contrastive learning of visual representations,” in *International Conference on Machine Learning (ICML’20)*, 2020, pp. 1597–1607.
- [45] J.-B. Grill, F. Strub, F. Altché, Tallec *et al.*, “Bootstrap your own latent a new approach to self-supervised learning,” vol. 33, pp. 21 271–21 284, 2020.
- [46] J. Zbontar, L. Jing, I. Misra, Y. LeCun, and S. Deny, “Barlow twins: Self-supervised learning via redundancy reduction,” in *Proceedings of the 38th International Conference on Machine Learning (ICML’21)*, 2021, pp. 12 310–12 320.
- [47] T. Hua, W. Wang, Z. Xue, S. Ren, Y. Wang, and H. Zhao, “On feature decorrelation in self-supervised learning,” in *Proceedings of the IEEE/CVF International Conference on Computer Vision (CVPR’21)*, 2021, pp. 9598–9608.
- [48] L. Jing, P. Vincent, Y. LeCun, and Y. Tian, “Understanding dimensional collapse in contrastive self-supervised learning,” in *Proceedings of the 10th International Conference on Learning Representations (ICLR’22)*, 2022.
- [49] Y. Zhang, H. Zhu, Z. Song, P. Koniusz, and I. King, “Spectral feature augmentation for graph contrastive learning and beyond,” in *Proceedings of the 37th AAAI Conference on Artificial Intelligence (AAAI-23)*, 2023, pp. 11 289–11 297.
- [50] X. Guo, Y. Wang, T. Du, and Y. Wang, “Contranorm: A contrastive learning perspective on oversmoothing and beyond,” in *Proceedings of the 11th International Conference on Learning Representations (ICLR’23)*, 2023.
- [51] H. Chen, V. Lai, H. Jin, Z. Jiang, M. Das, and X. Hu, “Towards mitigating dimensional collapse of representations in collaborative filtering,” *arXiv preprint arXiv:2312.17468*, 2023.



**Shaowen Peng** is an assistant professor at the Department of Information Science, NARA Institute of Science and Technology. His research interests span recommender systems and graph learning. He has published several papers in premier journals and conferences including TOIS, SIGIR, CIKM, and KDD.



**Kzunari Sugiyama** is a professor at Osaka Seikei University. Before joining Osaka Seikei University, he was an associate professor at Kyoto University from 2019 to 2023. He was also a research fellow at National University of Singapore from 2009 to 2019 (a senior research fellow from 2015 to 2019, a visiting scholar at Pennsylvania State University in 2014). He received his Ph.D. in Engineering from Nara Institute of Science and Technology in 2004. Prior to that, he received his B.Eng and M.Eng degrees from Yokohama National University in 1998 and 2000, respectively. His research interests include information retrieval, digital libraries, and natural language processing.



**Xin Liu** is a chief senior researcher with the Artificial Intelligence Research Center, National Institute of Advanced Industrial Science and Technology, Japan. He received the Ph.D. degree in computer science from Tokyo Institute of Technology. His research interests include machine learning and data mining for graph data, especially graph analysis, graph learning, network science, and web recommendations. He is a member of the editorial boards of the *Journal of Intelligent Information Systems* and *Intelligent Data Analysis*.



**Tsunenori Mine** received the B.E. degree in computer science and computer engineering and the M.E. and D.E. degrees in information systems from Kyushu University, in 1987, 1989, and 1993, respectively. He is currently an Associate Professor with the Department of Advanced Information Technology, Faculty of Information Science and Electrical Engineering, Kyushu University. His research interests include developing real services using artificial intelligence techniques, in particular, natural language processing, text mining, data mining, recommendation, and multiagent systems.